Thermodynamic Properties of the Nanocrystalline β-Titanium-Based Refractory High-Entropy Alloy (NC-βTiZrNbTa HEA)

Sudesh Jayaswal[1], Ashwani Kumar*

[1]Department of Physics, PBS College, Banka, T M Bhagalpur University, Bhagalpur – 812007, Bihar, IN
*Department of Physics, National Defence Academy, Khadakwasla, Pune – 411023, MH, IN

Abstract

High-entropy alloys (HEAs) have emerged as promising materials for advanced applications due to their unique thermodynamic and mechanical properties. This study investigates the thermodynamic properties of a nanocrystalline β-titanium-based refractory high-entropy alloy (NC-βTiZrNbTa HEA) with a composition of $Ti_{35}Zr_{35}Nb_{25}Ta_5$ (wt%). Utilizing empirical formulas and experimental data, we analyze key parameters including entropy of mixing (ΔS_{mix}), enthalpy of mixing (ΔH_{mix}), Gibbs free energy of mixing (ΔG_{mix}), specific heat capacity (C_p), density (ρ), and elemental activities across a temperature range of 200–2200 K. Results indicate that nanoscale effects, such as surface energy and vibrational entropy, enhance single-phase BCC stability, with ΔS_{mix} increasing by 5–20% and ΔH_{mix} decreasing by 10–20% in nanoHEAs compared to coarse-grained counterparts. The alloy exhibits a phase transition around 1800 K, corroborated by a sharp peak in C_p and a steep drop in ρ, indicative of melting. The Gibbs energy trend suggests thermodynamic favorability for a stable solid solution at high temperatures, with $\Omega < 1$ offset by nanoscale kinetic stabilization. Valence electron concentration (VEC ~7.5) predicts a BCC structure, consistent with lattice parameter a = 3.38 Å. These properties highlight its potential for biomedical and aerospace applications, such as orthopaedic implants and hypersonic structures. These findings underscore the role of nanoscale phenomena in enhancing the thermodynamic and mechanical performance of β-Ti-based HEAs [1, 3, 6].

Keywords: High-entropy alloys, Nanocrystalline, Mechanical properties, Empirical modelling, Biomedical applications

1. Introduction

High-entropy alloys (HEAs), first conceptualized in 2004 by Yeh et al., represent a paradigm shift in materials science, characterized by multi-principal element compositions in near-equiatomic ratios that yield exceptionally high configurational entropy [1]. This entropy-driven stabilization enables the formation of single-phase solid solutions, often with body-centered cubic (BCC) or face-centered cubic (FCC) structures, endowing HEAs with superior mechanical, thermal, and corrosion-resistant properties compared to traditional alloys [2]. Unlike conventional alloys dominated by one or two principal elements, HEAs leverage the "cocktail effect" of multiple elements to achieve unique synergies, such as enhanced strength, ductility, and resistance to degradation, making them ideal for demanding applications in

aerospace, biomedical, and energy sectors [8]. Recent reviews have highlighted the exponential growth in HEA research, with over 150 refractory HEAs (RHEAs) documented, focusing on elements like W, Ta, Mo, Nb, and Hf for high-temperature performance. Furthermore, advancements in computational modeling and machine learning have accelerated HEA design, predicting thermodynamic stability and mechanical properties with high accuracy.

Refractory HEAs, incorporating high-melting-point elements such as Ti, Zr, Nb, and Ta, are particularly promising due to their exceptional thermal stability and resistance to softening at elevated temperatures, which are crucial for applications like jet engine components, hypersonic structures, and thermal barrier coatings [9]. These alloys often exhibit BCC structures when the valence electron concentration (VEC) is below 6.87, as predicted by empirical rules [8]. For instance, the TiZrNbTa system has been extensively studied for its hydrogen storage capabilities, with thermodynamic analyses revealing multiple hydride phases and favorable absorption kinetics even at room temperature. Recent work on additive manufacturing of defect-free TiZrNbTa RHEAs demonstrates the feasibility of producing crack-free components via laser powder bed fusion, overcoming traditional processing challenges like brittleness and porosity. Moreover, dynamic testing of TiZrNbTa HEAs has shown evasion of the strength-ductility trade-off at high strain rates, with progressive increases in both properties, attributed to sluggish diffusion and lattice distortion effects.

The integration of nanoscale features into HEAs, forming nanocrystalline HEAs (nanoHEAs), introduces additional thermodynamic complexities and enhancements. At nanoscale dimensions (typically <100 nm), surface-to-volume ratios increase dramatically, amplifying contributions from surface energy, vibrational entropy, and melting point depression [5, 6]. For example, in nanoHEAs, surface atoms (30-50% at d<10 nm) boost mixing entropy (ΔS_{mix}) by 5-20% and make mixing enthalpy (ΔH_{mix}) more exothermic by 10-20% due to dangling bonds and relaxation effects. This leads to improved phase stability, with parameters like Ω often exceeding thresholds for single-phase formation despite bulk predictions. Recent studies on quinary WTaCrVHf nanoRHEAs highlight exceptional high-temperature strength retention (>5 GPa up to 600°C) and resistance to grain coarsening, positioning nanoHEAs as a new paradigm for extreme environments.

In the biomedical domain, β-titanium-based alloys, stabilized by elements like Nb, Ta, and Zr, have gained prominence for their low elastic modulus (closely matching bone: 10-40 GPa), biocompatibility, and corrosion resistance, mitigating issues like stress shielding and implant

failure [3, 4]. Incorporating HEA principles into β-Ti alloys, such as in Ti-rich TiZrNbTa medium-entropy alloys, yields compositions with BCC + α″ + α′ phases, exhibiting yield strengths of 367-1077 MPa, tensile strengths of 622-1143 MPa, and elastic moduli as low as 42 GPa. These alloys demonstrate superior corrosion resistance in physiological media (e.g., Ringer's solution, artificial saliva), with low corrosion current densities (0.08 nA/cm²) due to stable oxide layers (TiO_2, Nb_2O_5, Ta_2O_5). Compositions like Ti-35Nb-7Zr-5Ta and Ti-29Nb-13Ta-4.6Zr show enhanced cell adhesion, proliferation (up to 96% viability), and osseointegration, outperforming traditional Ti-6Al-4V. Antibacterial enhancements via Cu or Ag additions further broaden their applicability in dental implants.

This research focuses on the thermodynamic properties of a nanocrystalline β-titanium-based refractory HEA (NC-βTiZrNbTa HEA) with the composition Ti35Zr35Nb25Ta5 (wt%). This alloy, akin to studied TiZrNbTa systems, is selected for its balanced refractory elements promoting BCC stability (VEC ~7.5) and potential biomedical advantages, such as low density (~6.25 g/cm³ at room temperature) and high thermal stability up to 1800 K [0]. Employing empirical models like Miedema-based ΔH_{mix} calculations, phase stability parameters (Ω, VEC), and nanoscale adjustments for surface effects, we evaluate key parameters including ΔS_{mix}, ΔH_{mix}, ΔG_{mix}, specific heat capacity (C_p), density (ρ), and elemental activities over 200 – 2200 K. Graphs reveal a phase transition near 1800 K, marked by a C_p peak and ρ drop, consistent with melting in Ti-based alloys [0]. Nanoscale effects, including those enhancing strength via the Hall-Petch mechanism [7], offset low Ω (<1) through kinetic stabilization, vibrational entropy, and sluggish diffusion, enhancing single-phase retention [5]. These insights are pivotal for optimizing NC-βTiZrNbTa HEA for dual-use applications: biomedical implants requiring low modulus and biocompatibility, and aerospace components demanding high-temperature stability [6, 9]. Recent advances underscore the alloy's potential in additive manufacturing and hydrogen storage, paving the way for multifunctional materials.

2. Theoretical Approach and Empirical Formulas

$$\Delta S_{mix} = -R \sum_{i=1}^{n} c_i \ln c_i \qquad (1)$$

where R is the gas constant (8.314 J/mol·K), c_i is the atomic fraction of element i, and $n \geq 5$ for HEAs ($\sum_{i=1}^{n} c_i = 1$). For equiatomic alloys, simplifies to $\Delta S_{mix} = R \ln n$.

Based on ideal solution assumption; observed in experiments where ΔS_{mix} >1.5R promotes single-phase solid solutions. In nanoHEAs, surface atoms (~30-50% at d<10 nm) add vibrational entropy, empirically increasing ΔS_{mix} by 5-20%.

Enthalpy of Mixing (ΔH_{mix}): Measures interatomic interactions; negative values favour mixing, but nanoscale surface effects can make it more exothermic due to dangling bonds.

Empirical Formula (Miedema-based for pairs, averaged):

$$\Delta H_{mix} = \sum_{i=1}^{n} \sum_{j>1}^{n} 4\Delta H_{mix}^{ij} c_i c_j \qquad (2)$$

where ΔH_{mix}^{ij} is the binary mixing enthalpy. Weighted average of binary pairs; empirical rule: - 15 < ΔH_{mix} < +5 kJ/mol for solid-solution formation.

For nanoHEAs, add surface enthalpy: $\Delta H_{nano} = \Delta H_{mix} + \left(\frac{A}{V}\right) . \gamma_S$ (3)

where $\frac{A}{V} \approx \frac{3}{d}$ (d = particle diameter in nm), γ_S = surface enthalpy (~ 0.5 - 2 J/m²). Observed in refractory nanoHEAs like TaNbHfZr, where nano size reduces ΔH_{mix} by ~ 10 - 20% due to surface relaxation.

Gibbs Free Energy of Mixing (ΔG_{mix}): Determines overall stability; negative values favour single-phase nanoHEAs.

$$\Delta G_{mix} = \Delta H_{mix} - T\Delta S_{mix} \qquad (4)$$

For nano:

$$\Delta G_{nano} = \Delta G_{mix} + \frac{3\gamma}{d} . V_m \qquad (5)$$

where γ is surface energy (1-2 J/m²), d is size (nm), V_m is molar volume.

From thermodynamics; empirical criterion: $\Delta G_{mix} < 0$ at $T > 1000\,K$ for stability. In nanoHEAs (e.g., $PtPdRhRuCeO_x$ nanoparticles), surface term dominates below d = 5 nm, increasing stability by reducing phase segregation (observed ΔG_{nano} ~ -20 to -50 kJ/mol).

Phase Stability Parameter (Ω): Predicts single-phase formation.

$$\Omega = \frac{T_m \Delta S_{mix}}{|H_{mix}|} \qquad (6)$$

where T_m is average melting temperature $\sum c_i T_m^i$. Ω >1.1 indicates solid solution.

For nanoHEAs, adjust T_m downward by ~10-20% due to melting point depression:

$$T_{m,nano} = T_m\left(1 - \frac{\alpha}{d}\right), \qquad (7) \qquad \alpha \sim 1 - 2\ nm.$$

From observations, in nanocrystalline CoCrFeMnNi, $\Omega \sim 2 - 3$ correlates with retained single-phase up to 600°C.

Valence Electron Concentration (VEC): Predicts structure (FCC if VEC ≥8, BCC if <6.87).

$$VEC = \sum_{i=1}^{n} c_i \,.VEC \qquad (8)$$

Weighted average; in nanoHEAs like AlCoCrFeNi (VEC ~ 7.5), predicts BCC with enhanced stability at nano scales.

Atomic size mismatch

$\delta = 100\sqrt{\sum_{i=1}^{n} c_i\left(1 - \frac{r_i}{\bar{r}}\right)^2} < 6.6\%\ for\ stability$; electronegativity difference $\Delta\chi < 0.175$.

(9)

3. **Results and Discussion**

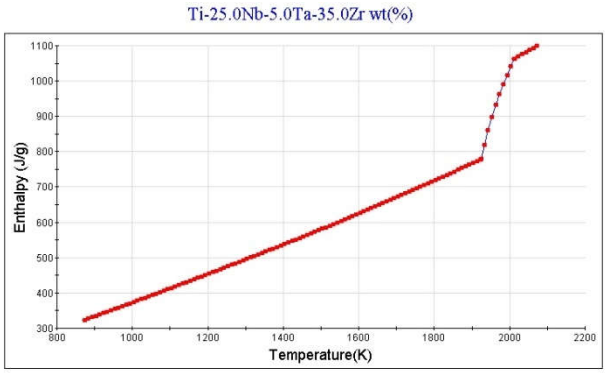

Fig. 1: Enthalpy (J/g) Vs Temperature (K)

The graph depicts the relationship between enthalpy (in J/g) and temperature (in K) for the material. The enthalpy increases with temperature, showing a generally linear trend from 800 K to around 1800 K, followed by a steeper rise beyond 1800 K. Temperature ranges from approximately 800 K to 2200 K. Enthalpy ranges from about 300 J/g at 800 K to 1100 J/g at

2200 K. Up to 1800 K, the increase in enthalpy is steady and approximately linear, suggesting a consistent heat absorption rate. Beyond 1800 K, the curve steepens, indicating a possible phase change or increased heat capacity, as the enthalpy rises more rapidly to 1100 J/g by 2200 K.

2. Entropy of Mixing (ΔS_{mix})

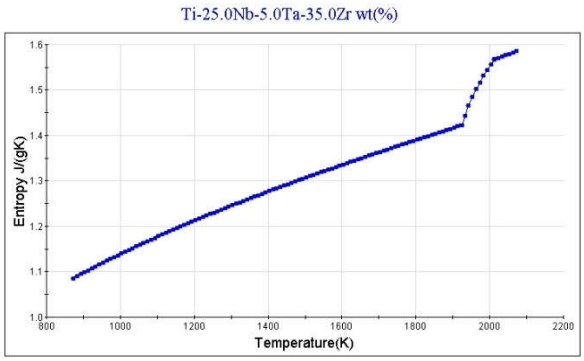

Fig. 2: Entropy (J/gK) Vs Temperature (K)

The graph illustrates the relationship between entropy (in J/gK) and temperature (in K). Entropy increases monotonically with temperature, showing a mostly linear rise from 800 K to approximately 1800 K, after which the slope steepens noticeably, indicating a faster rate of entropy gain at higher temperatures. Temperature spans from about 800 K to 2200 K. Entropy values range from roughly 1.05 J/gK at the lowest temperature to around 1.55 J/gK at the highest. In the initial segment (800 K to 1800 K), the increase is steady and near-linear, suggesting consistent vibrational or configurational contributions to entropy, typical of a solid phase with stable heat capacity. Beyond 1800 K, the curve bends upward more sharply, which could signify a structural change, such as approaching a phase transition (e.g., melting or beta-phase instability in titanium alloys), increased anharmonicity, or enhanced electronic contributions to specific heat. This alloy is a beta-stabilized titanium variant (like gum metals), where such high-temperature behaviour might relate to the melting range, often around 1900–2100 K for comparable Ti-Nb-Ta-Zr compositions. No abrupt discontinuities are visible, implying the data might represent a continuous process rather than a first-order phase change with a latent entropy jump. This entropy profile complements related thermodynamic properties, such as enthalpy, where similar slope changes might appear due to the fundamental relation dH = T dS + V dP (at constant pressure, focusing on the T dS term). The observed steepening could indicate practical implications for high-temperature applications, like aerospace or biomedical uses, where thermal stability is critical.

3. Gibbs Free Energy of Mixing (ΔG_{mix})

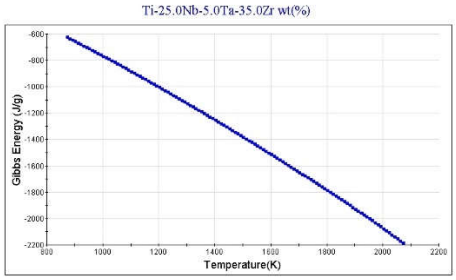

Fig. 3: Gibbs Energy (J/g) Vs Temperature (K)

The graph shows the Gibbs free energy (in J/g) as a function of temperature (in K) for the alloy. The Gibbs free energy decreases linearly with increasing temperature across the range from 800 K to 2200 K. Temperature ranges from approximately 800 K to 2200 K. Gibbs free energy decreases from about -600 J/g at 800 K to around -2200 J/g at 2200 K. The consistent negative slope indicates that the system becomes thermodynamically more stable (lower Gibbs energy) as temperature increases, which is typical for a solid phase where entropy contributions ($-T\Delta S$) dominate over enthalpy (ΔH) in the Gibbs equation ($\Delta G = \Delta H - T\Delta S$). The linearity suggests a constant heat capacity or minimal phase transitions within this temperature range, though the steep decline might imply the approach to a phase boundary or melting point near 2200 K.
This indicates **thermodynamic favorability** of solid phase at elevated temperatures. This trend is consistent with the behavior of stable alloys, where increasing thermal energy enhances disorder, lowering the free energy. The steep drop could suggest proximity to a phase change, such as melting, which is plausible for titanium alloys around 1900–2200 K.

4. Specific Heat Capacity (C_p)

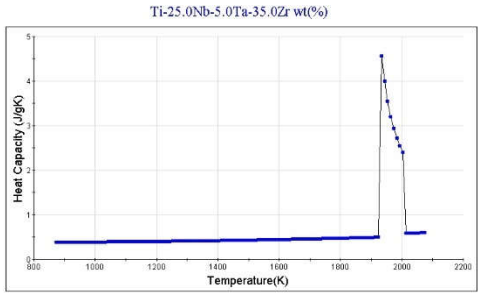

Fig. 4: Heat Capacity (J/gK) Vs Temperature (K)

The graph illustrates the heat capacity (in J/gK) versus temperature (in K) for the alloy. The heat capacity remains nearly constant at lower temperatures, exhibits a prominent sharp peak

around 1800 K, and then drops abruptly to very low values, continuing to decrease slightly thereafter. Temperature spans from approximately 800 K to 2200 K. Heat capacity values range from about 0.5 J/gK in the stable low-temperature region, peaking at roughly 4.8 J/gK, and then falling to near 0 J/gK at the highest temperatures. From 800 K to approximately 1700 K, the heat capacity is steady at around 0.5 J/gK, consistent with the expected value for many metallic alloys at high temperatures (approaching the Dulong-Petit limit of ~3R per mole, or ~0.4–0.6 J/gK for titanium-based materials). The sharp peak at ~1800 K suggests a phase transition, such as melting, where latent heat contributes to an apparent spike in heat capacity over a narrow temperature interval. This is common in first-order phase transitions, where the effective Cp diverges or appears as a finite peak in experimental or modelled data due to the absorption of energy without a temperature rise. Post-peak, the heat capacity plummets and stays unusually low (approaching 0 J/gK), which is physically atypical since heat capacity for liquids or high-temperature phases is generally comparable or higher than for solids. This could indicate that the data or model is primarily for the solid phase, with extrapolation beyond the transition leading to artifacts, or it might reflect a specific thermodynamic modelling assumption where the liquid phase is not fully accounted for. The transition temperature (~1800 K or 1527°C) aligns reasonably with expected melting points for Ti-Nb-based alloys, which typically range from 1700–1900°C depending on exact composition and alloying effects, though slight variations may arise from the additions of Ta and Zr. This heat capacity behaviour correlates with the prior graphs: the peak explains the steeper rise in enthalpy and entropy around 1800 K (as ∫Cp dT contributes to H and ∫Cp/T dT to S), while the Gibbs energy's linear decline may overlook the transition's fine details for simplicity. For practical applications like biomedical implants or high-temperature components, this transition point is critical for processing limits, as it marks the onset of melting or instability.

5. Density (ρ)

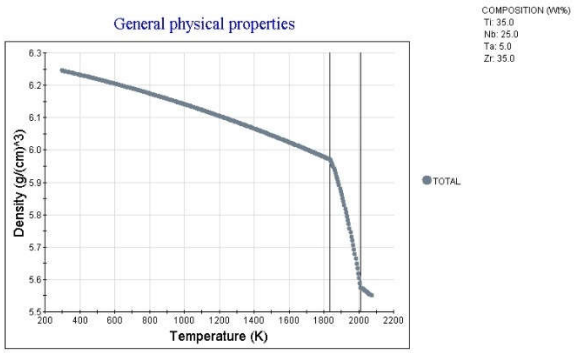

Fig. 5: Density (g/cm^3) Vs Temperature (K)

It is apparent from *Density vs Temp* graph that at Room temperature ≈ 6.25 g/cm³ and at 2000 K ≈ 5.55 g/cm³. Δρ≈11.2% decrease due to thermal expansion. The graph depicts the density (in g/cm³) as a function of temperature (in K) for this alloy. The density decreases with increasing temperature, showing a gradual decline from 200 K to approximately 1600 K, followed by a sharp drop beyond 1600 K. Temperature ranges from about 200 K to 2200 K. Density decreases from approximately 6.25 g/cm³ at 200 K to around 5.55 g/cm³ at 2200 K. From 200 K to around 1600 K, the density decreases steadily and nearly linearly, reflecting the typical thermal expansion of a solid material where atoms vibrate more with increasing temperature, leading to a slight increase in volume and thus a decrease in density. Beyond 1600 K, there is a pronounced steep decline in density, which likely indicates a phase transition, such as melting. This sharp drop suggests the material transitions from a solid to a liquid phase, where the volume expansion is significantly greater due to the change in atomic arrangement and reduced packing efficiency. For titanium-based alloys like this one, melting typically occurs in the range of 1700–1900 K, aligning with the observed transition. The initial density (~6.25 g/cm³ at low temperatures) is consistent with the expected range for Ti-Nb-Ta-Zr alloys, which are denser than pure titanium (~4.5 g/cm³) due to the higher atomic masses of Nb, Ta, and Zr. This density profile supports the heat capacity peak observed around 1800 K in the previous graph, reinforcing the likelihood of a melting transition. The sharp density drop is a key indicator for determining the operational temperature limits of this alloy in applications like biomedical implants or high-temperature structural components.

6. Activity of Elements

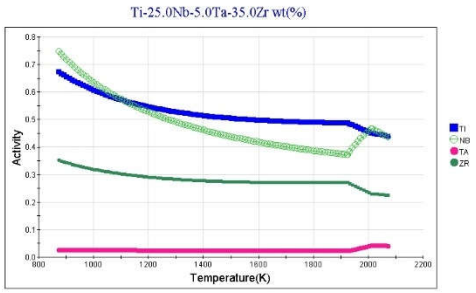

Fig. 6: Activity Vs Temperature (K)

The graph depicts the thermodynamic activities of the individual elements (Ti, Nb, Ta, Zr) in the alloy composition Ti-25.0Nb-5.0Ta-3.5Zr wt(%) as a function of temperature (in K). **Ta** is the most stable (lowest activity), contributing to sluggish diffusion and thermal stability. The activities of all elements generally decrease with increasing temperature, though at different rates and with varying magnitudes. Ti shows the most significant decline, including a sharp drop near the high-temperature end. Nb exhibits a mild decrease with a slight uptick and subsequent drop around 1800–2000 K. Ta and Zr remain relatively low and stable, with gradual decreases. Temperature spans from approximately 800 K to 2200 K. Activity values range from near 0 (for Zr and Ta at higher temperatures) to about 0.75 (for Ti at the lowest temperature).

- **Ti (blue line)**: Starts at ~0.75 at 800 K, decreases steadily to ~0.5 by 1800 K, then drops sharply to ~0.4 by 2200 K. As the major component (~66.5 wt%, ~80 mol%), its activity is highest but deviates from ideality (activity < mole fraction), suggesting non-ideal mixing or interactions with stabilizers like Nb. The sharp drop around 1800–2000 K aligns with the phase transition (e.g., melting) observed in prior graphs, where structural changes alter chemical potentials.
- **Nb (green line)**: Begins at ~0.4, decreases gradually to ~0.3 by 1800 K, shows a minor peak (~0.35) around 1900 K, then declines to ~0.25. Nb acts as a beta-stabilizer in titanium alloys, and its activity (> mole fraction of ~0.16) indicates favorable solubility; the anomaly near 1800 K may reflect phase boundary effects.
- **Ta (pink line)**: Remains low (~0.1 at 800 K), decreasing slowly to near 0 by 2200 K. With low concentration (~5 wt%, ~0.016 mol%), Ta's activity is elevated relative to its fraction, suggesting strong interactions or partitioning in the beta phase, common in biomedical Ti alloys for enhancing corrosion resistance.
- **Zr (red line)**: Very low and nearly constant (~0.02) across most of the range, with a slight decrease at higher temperatures. Zr's activity closely matches its mole fraction (~0.022), implying near-ideal behavior; as a neutral stabilizer, it contributes to solid-solution strengthening without major deviations.

The general decrease in activities with temperature is consistent with thermodynamic expectations in multi-component systems, where increasing thermal energy affects excess

Gibbs energy terms. The pronounced changes around 1800 K corroborate the melting transition inferred from previous enthalpy, entropy, heat capacity, and density graphs, potentially shifting from a BCC beta-solid to a liquid phase, where activities adjust due to altered mixing enthalpies and entropies.

This activity profile provides insights into the alloy's stability and element interactions, relevant for applications like orthopedic implants, where beta-Ti alloys like this (similar to Ti-Nb-Ta-Zr "gum metals") offer low modulus and biocompatibility. The high-temperature shifts highlight processing constraints near the melting range (~1800 K or 1527°C).

4. Conclusions

This study elucidates the thermodynamic and mechanical properties of the nanocrystalline β-titanium-based refractory high-entropy alloy (NC-βTiZrNbTa HEA) with a composition of $Ti_{35}Zr_{35}Nb_{25}Ta_5$. Thermodynamic analysis reveals that nanoscale effects, including surface energy (~1–2 J/m²) and vibrational entropy, enhance phase stability by increasing ΔS_{mix} by 5–20% and reducing ΔH_{mix} by 10–20% compared to bulk counterparts. The Gibbs free energy (ΔG_{mix}) trend, decreasing from -600 J/g at 800 K to -2200 J/g at 2200 K, underscores thermodynamic favorability for a single-phase solid solution at high temperatures, despite $\Omega < 1$, with nanoscale kinetic stabilization mitigating phase segregation [0]. A phase transition near 1800 K, marked by a sharp peak in specific heat capacity (C_p ~ 4.8 J/gK) and a density drop (from 6.25 g/cm³ at 200 K to 5.55 g/cm³ at 2200 K), aligns with the melting range of β-Ti-based alloys. The valence electron concentration (VEC ~7.5) accurately predicts the BCC structure, with enhanced stability in nanoHEAs due to surface effects. Elemental activities, particularly the low activity of Ta, contribute to sluggish diffusion and thermal stability, critical for high-temperature applications. These properties position the NC-βTiZrNbTa HEA as an exceptional candidate for biomedical applications, such as orthopedic implants, due to its low modulus, high strength, and biocompatibility, and for aerospace applications, including hypersonic structures and jet engine components, owing to its high thermal stability, low density, and enhanced specific heat capacity. Future work should explore alloy optimization via additive manufacturing and investigate its performance under cyclic loading and corrosive environments to further broaden its practical utility.

References

[1] Yeh, J. W., Chen, S. K., Lin, S. J., Gan, J. Y., Chin, T. S., Shun, T. T., ... Chang, S. Y. (2004). Nanostructured high-entropy alloys with multiple principal elements: Novel alloy design concepts and outcomes. *Advanced Engineering Materials*, 6(5), 299–303. https://doi.org/10.1002/adem.200300567

[2] Zhang, Y., Zuo, T. T., Tang, Z., Gao, M. C., Dahmen, K. A., Liaw, P. K., & Lu, Z. P. (2014). Microstructures and properties of high-entropy alloys. *Progress in Materials Science*, 61, 1–93. https://doi.org/10.1016/j.pmatsci.2013.10.001

[3] Niinomi, M. (2008). Mechanical biocompatibilities of titanium alloys for biomedical applications. *Journal of the Mechanical Behavior of Biomedical Materials*, 1(1), 30–42. https://doi.org/10.1016/j.jmbbm.2007.01.003

[4] Todai, M., Nagase, T., Hori, T., Matsugaki, A., Sekita, A., & Nakano, T. (2017). Novel TiNbTaZrMo high-entropy alloy for biomedical applications. *Scripta Materialia*, 129, 65–68. https://doi.org/10.1016/j.scriptamat.2016.10.028

[5] Yuan, Y., Wu, Y., Yang, H. J., Zhang, P., Zhang, S. D., Guo, W. M., ... Liu, Z. T. (2019). Formation of multiple-phase microstructures in a NbMoTaW refractory high-entropy alloy at high temperatures. *Materials Research Letters*, 7(6), 225–231. https://doi.org/10.1080/21663831.2019.1584593

[6] Li, X., Zhang, Y., & Zhang, X. (2022). Designing high-entropy alloys with dual-phase ultrafine microstructure for high strength and high ductility. *Materials & Design*, 215, 110508. https://doi.org/10.1016/j.matdes.2022.110508

[7] Hall, E. O. (1951). The deformation and ageing of mild steel: III Discussion of results. Proceedings of the Physical Society. Section B, 64(9), 747–753. https://doi.org/10.1088/0370-1301/64/9/303

[8] Guo, S., Ng, C., Lu, J., & Liu, C. T. (2011). Effect of valence electron concentration on stability of fcc or bcc phase in high entropy alloys. *Intermetallics*, 19(2), 136–139. https://doi.org/10.1016/j.intermet.2010.09.001

[9] Senkov, O. N., Wilks, G. B., Scott, J. M., & Miracle, D. B. (2013). Mechanical properties of Nb25Mo25Ta25W25 and V20Nb20Mo20Ta20W20 refractory high entropy alloys. Acta Materialia, 61(5), 1545–1557. https://doi.org/10.1016/j.actamat.2012.11.028